

Aseptic Efficiency of Zinc Oxide-Carbonized Zobo (*Hibiscus Sabdariffa*) Waste Nanocomposites and Magnesium-Zinc Binary Oxide Nanocomposite on Bacteria as well as Removal efficiency on Cadmium and Nickel in Contaminants Water

O. MOSES* and S. O. OMOYE

Department of Chemistry, Faculty of Physical Sciences, University of Benin, Nigeria

Received: 23/12/2024 **Accepted:** 02/03/2025

Abstract

Human activities have immensely contributed to pollutants in water bodies such as heavy metals, organic and pathogenic microorganisms. This study was aimed to synthesize and investigate the aseptic efficacy of ZnO-carbonized zobo waste nanocomposite (ZOCZWNC) and Mg-Zn binary oxide (Mg-ZnBO) nanocomposite on *Salmonella typhi* – gram negative organism and *Staphylococcus aureus* – gram positive organism as well as removal of cadmium and nickel ions from contaminated water. Mg-Zn binary oxide (Mg-ZnBO) Nanocomposite and ZnO-carbonized zobo waste nanocomposite (ZnOCZWNC) was prepared and characterized. Adsorption investigation was done using adsorption isotherm and the aseptic efficiency of ZnOCZWNC and MgZnBO nanocomposites was studied using turbidimetric method. Maximum sorption capacity of cadmium onto ZnOCZWNC and Mg-ZnBO was 9.11mg/g and 192.31mg/g respectively and 714.29 mg/g and 416.67 mg/g in that order for nickel ions. The average crystallite size of ZnOCZWNC and MgZnBO was 40.94 nm and 59.42nm respectively. The treated samples experienced a steady decrease in the population of *Staphylococcus* and *Salmonella* within 2hrs, after about 2hrs, the samples of *staphylococcus* and *salmonella* treated with ZnOCZWNC continued to show continuity in its aseptic effect at decreasing the population of the bacteria with time. The *staphylococcus* and *salmonella* sample treated with MgZnBO experienced a slightly steady drop in the effectiveness of the nanocomposite after same period. The ZnOCZWNC removed nickel ions more effectively compared to Mg-ZnBO, conversely, MgZnBO removed cadmium ions more effectively compared to ZnOCZWNC. ZnOCZWNC was more efficient in drastically reducing the population of *staphylococcus* and *salmonella* in contaminated water.

Keywords: *Nanocomposites, Antibacterial activity, Binary Oxide, Heavy metal, Salmonella, Staphylococcus.*

1. INTRODUCTION

Human activities have in so many ways contributed to existence of pollutants in water for instance heavy metals, organic and pathogenic microorganisms due to improper handling and disposal of waste from industrial, domestic and mining activities. Heavy metals are hazardous pollutants due to their persistent, non-biodegradable and harmful effects. Heavy metals for instance cadmium as well as nickel are deleterious associated with lethal, mutagenic and cancer-causing properties (Renu and Kailash, 2022). Pathogenic bacteria such as *Salmonella typhi* (Gram-negative bacterium) and *Staphylococcus aureus* (Gram-positive bacterium) are biological pollutants resulting from poor hygiene. These bacteria are responsible for infectious diseases such as cholera, typhoid fever, diarrhea, gastrointestinal diseases in humans (Esonu *et al.*, 2021; Hassan *et al.*, 2022). In order to access improved water quality, it is pertinent to device an effective removal technique of these pollutant so as to safe guard human health and protect ecological environment (Geletu *et al.*, 2022). Antibacterial agents have been extensively used to combat the proliferation as well as amount of bacteria, but they come with various limitations such as antibacterial resistance, environmental pollution, high-cost and labour intensive processing methods. As such, there is medical as well as economical request for emergent new antibacterial agents in the form of a nanocomposite (Haque *et al.*, 2021; Rafiq *et al.*, 2024).

Likewise, efforts at removing heavy metals from polluted water has involved various technologies and approaches, including advanced water treatment processes like filtration, coagulation, chemical precipitation and ion exchange (Ahmed *et al.*, 2022; Fwangmun *et al.*, 2023). However, adsorption is considered the best treatment technique due to its high removal efficiency, cost-effectiveness, lesser energy consumption, strong practicality, high applicability, good operability, low waste generation and little harmfulness (Ambaye *et al.*, 2021; Naila *et al.*, 2022).

Despite substances for example activated carbon, silica gel, zeolite, biomass as well as activated charcoal had been exploited as adsorbents for heavy metals, nanomaterial such as nanocomposites and metals binary oxide nanoparticle possess promising values in heavy metals adsorption as well as removal of bacteria in water due to their chemical reactivity, large adsorption surface area, high porosity, enhanced structural properties, catalytic properties and chemical stability in solution (Subha *et al.*, 2018; Yu *et al.*, 2021). The dried reddish *Roselle* Hibiscus (*Hibiscus Sabdariffa*) flower (Figure 1) of the plant are commonly known

as zobo leaves in Nigeria and is used to make beverage (zobo drink). This study was aimed to synthesize and study the aseptic efficacy of ZnO-carbonized zobo waste nanocomposite (ZOCZWNC) and Mg-Zn binary oxide (Mg-ZnBO) nanocomposite on *Salmonella typhi* and *Staphylococcus aureus* as well as removal of cadmium (Cd^{2+}) and Nickel (Ni^{2+}) ions in simulated polluted water.



Figure 1: Roselle Hibiscus flower (*Hibiscus Sabdariffa*)

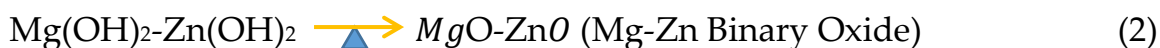
2. MATERIALS AND METHOD

2.1 Preparation of Mg-Zn Binary Oxide (Mg-ZnBO) Nanocomposite

Mg-Zn Binary oxide Nanocomposite was synthesized by chemical co-precipitation and thermal degradation method, take up from Faisal *et al.*, (2022) and Khine *et al.*, (2022) with slim modifications.

Solution A was prepared by dissolving 2.9g, zinc sulphate (ZnSO_4) in 2% PVA solution in 100ml distilled water in volumetric flask, and stirred to dissolve. Likewise, solution B was prepared by dissolving 2.47g of magnesium sulphate (MgSO_4) in 2% PVA solution in 100ml distilled water in volumetric flask, and stirred to dissolve. In preparing solution C, 0.82g sodium hydroxide (NaOH) was dissolved in 2% PVA solution in 100ml distilled water in a volumetric flask and stirred vigorously. Solution C was added drop wisely from the burette to an equivolume mixture of 25ml each of solution A and B in a 500 ml flat bottom flask, with continuous mixing. The reaction mixture was continuously agitated for 2hours on a magnetic agitator at a temperature of 90°C . The solution was allowed to calm down for 6 hours. The precipitate obtained was centrifuged and washed at least five times with distilled water with repeated centrifugation to get rid of leftover NaOH and Na_2SO_4 . The obtained precipitate was then dried in an oven at 100°C and lastly, the Mg-Zn binary oxide nanocomposite was got by calcining the magnesium-zinc mixed hydroxide ($\text{Mg}(\text{OH})_2\text{-Zn}(\text{OH})_2$) initially obtained at 950°C for 6hours. The chemical equation of the reaction is shown in equation 1 and 2:





2.2 Preparation of ZnO–Carbonized Zobo (*Hibiscus Sabdariffa*) waste Nanocomposite (ZnOCZWNC)

Dried *hibiscus Sabdariffa* flower zobo flower was obtained from Egor market and further dried for one week to eliminate moisture. The zobo flower waste obtained after extraction of beverage (zobo drink) was dried in an oven at 85°C for a week. The dried zobo waste obtained was carbonized in a muffle furnace (Carbolite, AAS 1110) at 300°C for 30 minutes. The carbonized waste was ground using a British milling machine and sieved with mesh size 40µm to get uniform particles.

ZnO–Carbonized Zobo (*Hibiscus Sabdariffa*) waste Nanocomposite (ZnOCZWNC) was prepared adopting Moses and Oyibo, (2022) method with slim modification. Solution A was made by dissolving 2.9g of zinc sulphate (ZnSO_4) in 2% PVA solution in 100ml distilled water in volumetric flask and stirred to dissolve, likewise, solution B was prepared by dissolving 0.82g of sodium hydroxide (NaOH) in 2% PVA solution in 100ml distilled water in a volumetric flask and agitated to dissolve. Solution B was added drop wisely from the burette to solution A in a 500 ml flat bottom flask, with stirring on a magnetic stirrer. The reaction mixture was continuously stirred for 1hour on a magnetic stirrer at a temperature of 90°C after which 1g of carbonized zobo waste (CZW) was added to the reaction mixture and was allowed to stir for another 2 hours. The reaction mixture was allowed to calm down for 24 hours. The resulting product was centrifuge and washed atleast 5 times. The resulting product was calcinated in a muffle furnace at 290°C for 90 minutes. After which the nanocomposite was taken out of the furnace and put in a desiccator for 12 hours. The chemical equation of the reaction is shown in equation 3, 4 and 5:



2.3 Characterization of the Nanocomposites

The prepared nanomaterials were characterized using Fourier Transform-Infra Red (FT-IR System, spectrum BX, PerkinElmer, England), Scanning electron microscopy (SEM; Phenom pro suite desktop scanning electron microscope) and x-ray diffraction (with X-Ray diffractometer, Schimadzu 6000 model).

2.4 Adsorbate Preparation, Adsorbent Adsorption Capacity and Efficiency Analysis

Simulated solution of cadmium and nickel contaminated water (adsorbates) were prepared from their respective BDH analytical grade salts. The concentration of

the cadmium ion and nickel ions in prepared solution was affirmed with use of atomic absorption spectrophotometer (AAS, Buck scientific model VGP-210). Cadmium and nickel ions removal efficiency using ZnOCZWNC and MgZBO nanocomposites was studied through batch adsorption experiments. Batch adsorption parameter such as time, pH, adsorbent dosage and initial concentration was systematically varied and controlled to understand the efficiency of ZnOCZWNC and MgZBO nanocomposites on the removal of cadmium and nickel. Equilibrium quantity of adsorbate adsorbed (adsorption capacities) as well as adsorption efficiency was determined using the equation 6 and 7 respectively (Ku'smirek *et al.*, 2021; Renu and Kailash, 2022):

$$q_e = \frac{(C_o - C_e)}{M} \times V \quad (6)$$

$$\%E = \frac{(C_o - C_e)}{C_o} \times 100 \quad (7)$$

Where q_e is the quantity of adsorbate adsorbed in mg/g of adsorbent; %E adsorption efficiency; C_o is the initial concentration of the metal ion prior to the adsorption process; C_e is the equilibrium concentration of the metal ion in the filtrate after adsorption process; M is mass of adsorbent and V is volume of solution in litre.

2.5 Adsorbent Adsorption Analysis Using Adsorption Isotherm

The graphical correlation between quantity of adsorbate adsorbed on the adsorbent's surface at equilibrium concentration of adsorbate in solution at constant temperature was investigated with the use of different adsorption isotherm models, Which helps to provides information about the nature of the contacts involving the adsorbent and adsorbates, as well as the affinity of the adsorbate for adsorbent surface (Ugrina *et al.*, 2023). Adsorption isotherm studies was carried out using Langmuir, Freundlich and Dubinin-Raduskevich adsorption isotherm models (equation 8, 9 and 10) to evaluate the data obtained so as to predict whether adsorption occurred uniformly on the active site and to quantifies and contrasts the capacity of different adsorbents; or the processes occurred on a multilayer sorption on a heterogeneous surfaces; or to assess the porosity of the adsorbent, the apparent energy of adsorption and mechanism of adsorption whether physiosorption or chemisorption respectively (Kalarikkandy *et al.*, 2022; Kesamsetty *et al.*, 2022). The linear equations of models are stated below:

$$\frac{1}{q_e} = \frac{1}{q_m} + \frac{1}{k_L q_m C_e} \quad (\text{Langmuir}) \quad (8)$$

$$\ln q_e = \frac{1}{n} \ln C_e + \ln K_f \quad (\text{Freundlich}) \quad (9)$$

$$\ln q_e = \ln q_m - \beta E^2 \quad (\text{Dubinin-Raduskevich}) \quad (10)$$

Where: C_e is the equilibrium concentration of the adsorbate ($\text{mg}\cdot\text{L}^{-1}$), q_e is the equilibrium adsorption capacity of the adsorbent ($\text{mg}\cdot\text{g}^{-1}$), q_m is the maximum sorption capacity (mg/g), k_L (L/mg) is adsorption equilibrium constant (L/mg) at a specified temperature linked to the energy of sorption, it is a direct evaluation of the intensity of adsorption process. The value of K_L is connected with dimensionless constant (Dewangan *et al.*, 2021; Ugrina *et al.*, 2023).

K_f and n are Freundlich constants, indicating adsorption capacity and adsorption intensity or surface heterogeneity indices respectively. $\frac{1}{n}$ which ranges between 0 and 1 (or n ranges between 1-10), is a measure of adsorption intensity or surface heterogeneity, If n lies between 1 and 10, this indicates a favorable sorption process. It become more heterogeneous as its value gets closer to zero. Whereas, value lower than unity indicates chemisorptions process, when $1/n$ is above one, it indicates cooperative adsorption (Yousefi-Limaee, *et al.*, 2023). β (mol^2/J^2) is activity coefficient constant which gives information on the mean free energy of adsorption per molecule of the adsorbate when it is transported to the surface of the adsorbent from infinity in the solution, E (J^2/mol^2) is related to the equilibrium concentration (C_e , mgL^{-1}) by the equation: $[RT \ln (1 + 1/C_e)]$. The apparent energy (E , kJ/mol) of adsorption per molecule of adsorbate (for taking away a molecule from its position in sorption space to infinity) from Dubinin-Radushkevich isotherm model can be calculated using the relation given below (equation 11):

$$E = (2\beta)^{-1/2} \quad (11)$$

The nature of sorption process can be predicted based on the E value. If $E < 8$ kJ/mol , the sorption is of a physical nature (physiosorption), for $8 < E < 16$ kJ/mol , the sorption occurred by ion exchange, however for $E > 8$ kJ/mol , the sorption is of a chemical nature (chemisorption) (Ugrina *et al.*, 2023).

2.6 Study of Aseptic Effect of ZnOCZWNC and MgZBO Nanocomposites

Evaluation of the aseptic effect of ZnOCZWNC and MgZBO nanocomposites on *Salmonella typhi* and *Staphylococcus aureus* was carried out using turbidimetric analysis, a process which helps to determine the decimation of the bacteria by the nanocomposite. This process, involves the use of incident beam of light from UV-Visible spectrophotometer through a sample in a cuvette and the intensity of the transmitted light was measured. The lower the light beam transmitted, the higher the amount of the bacterial available (or present) in the water sample and vice versa. A control standard without the antibacterial agent was also made to confirm the effectiveness of the antibacterial agent. The readings in transmittance were plotted against time.

Before analysing the aseptic efficiency of ZnOCZWNC and MgZBO nanocomposites against *Salmonella typhi* and *Staphylococcus aureus* using turbidimetric method, the bacterial strains were cultured under standard laboratory conditions by Enebeli Benneth Chukwudi, a Chief laboratory technologist and a specialist in the area of microbiology/plant pathology from the Department of Plant Biology and Biotechnology, University of Benin, Benin City. Clinically isolated bacteria on Petri dishes and prepared broth (nutrients) were obtained from University of Benin Teaching Hospital, Benin City. The nutrient broth were placed in two (2) flasks with double distilled water, sterilized and activated in a pressure pot. Each surface of bacteria was swabbed by a sterile cotton swab (swab stick) and dissolved in a beaker containing 5ml of sterilized water. A syringe was used to measure 5ml of the dissolved bacteria into each sample bottle appropriately labeled. Then 15ml of the broth was measured into each labeled sample bottle containing each bacteria specie. After which the nanocomposite material at the various concentrations were introduced into each sample bottle respectively at room temperature. Each sample bottle was incubated at 37°C for 24hours. After incubation, each sample bottle was taken for absorbance and transmittance measurement in the UV-Vis Spectrophotometer (JENWAY 6320D). The absorption spectrum of each sample is measured and noted at 0.5hr, 1hr, 1.5hr, 2hrs and 24 hrs minutes respectively.

3. RESULT AND DISCUSSION

3.1 Characterization of ZnO-Carbonized Zobo (*Hibiscus Sabdariffa*) Waste (ZnOCZWNC) and Mg-Zn Binary Oxide Nanocomposites.

The ZnO-carbonized zobo waste nanocomposite (ZnOCZWNC) and Mg-Zn binary oxide nanocomposite was characterized by means of FT-IR spectrometer, XRD Diffractometer and SEM microscope.

The FT-IR spectra revealed the presence of -OH group at a peak of 3841cm⁻¹, 3823, 3569 and 3327cm⁻¹ due to the presence of moisture and hydroxyl group on the ZnO-carbonized zobo waste. While the characteristic FT-IR spectra peak at 3905cm⁻¹-3324cm⁻¹ in Zn-Mg binary oxide was assigned to the O-H stretching vibration as a result of moisture. The spectra revealed availability of carboxylate on ZnOCZWNC at a peak of 1413cm⁻¹ and 1562cm⁻¹. The peak at 2002cm⁻¹ and 2024cm⁻¹ revealed the presence of ketenimine (-C=C=N-) and isothiocyanate (-N=C=N-). The N-H stretch at a peak of 3327 was attributed to secondary amine. The peak at 743cm⁻¹ and 881cm⁻¹ revealed the presence of mono and meta-disubstituted aromatic compound. Zn-O stretching of ZnO was observed at 717cm⁻¹ and 680 cm⁻¹ in the ZnOCZWNC nanocomposite. Zn-Mg stretching of Zn-Mg binary oxide at 992cm⁻¹ and 917cm⁻¹ indicating the presence of Zn, Mg, and O within ZnO-MgO nanocomposites (Figure 2).

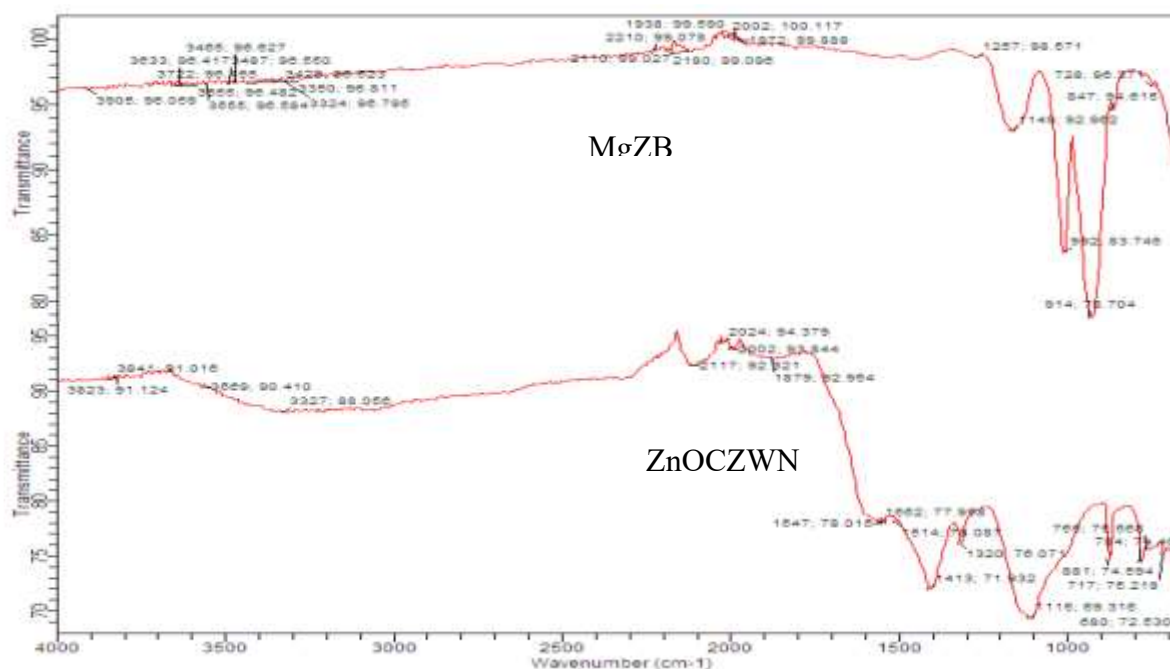


Figure 2: FT-IR Spectra for Mg-Zn Binary Oxide nanocomposite (MgZBO) and ZnO-Carbonized Hibiscus Waste Nanocomposite. (ZnOCZWNC)

The surface morphology of the ZnO-Carbonized zobo Waste Nanocomposite was examined using scanning electron microscopy. SEM micrographs was obtained using an accelerating voltage of 10 kV at x1,500 magnification. SEM micrographs clearly revealed that ZnO-Carbonized zobo waste nanocomposite had a smooth surface and variety of irregular pores. It has a crystalline texture in look. The SEM microgram of the Mg-Zn binary oxide nanocomposite revealed under the same SEM conditions had a smooth sheet like flaky surface and crystalline look with a lesser amount of irregular pores (Figure 3A and 3B).

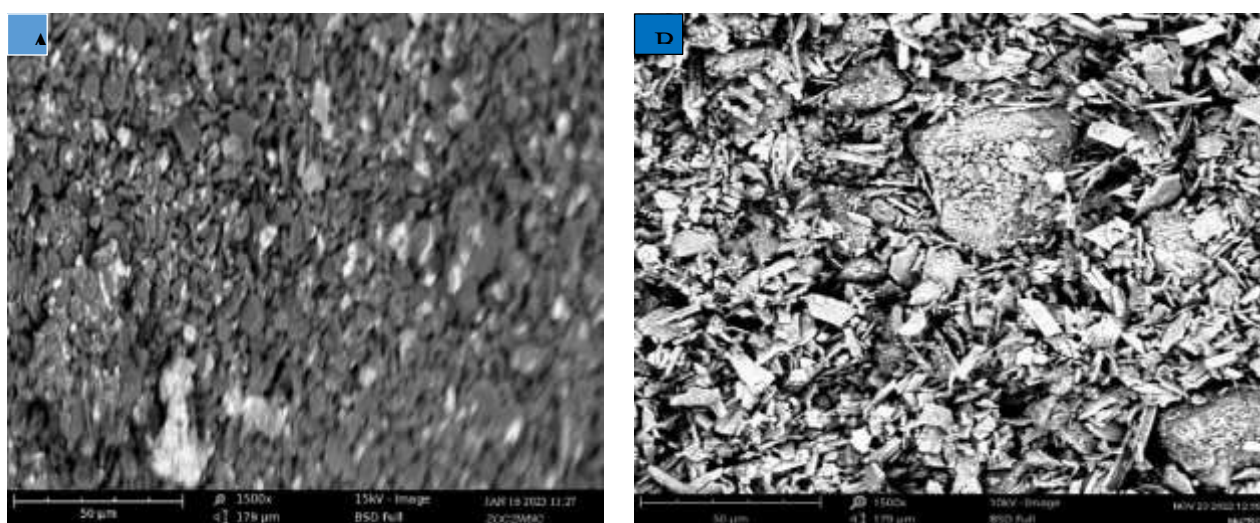


Figure 3: SEM image for ZnO-Carbonized Zobo Waste Nanocomposite (ZnOCZWNC)-A and SEM image for MgO-ZnO Binary Oxide nanocomposite (MgZBO)-B

X-ray diffractogram of the ZnOCZWNC and MgZBO nanocomposites (Figure 4) was obtained using the EMPYREAN-NGRL X-ray diffractometer with Cu K-Alpha radiation: 0.15406nm (1.5406Å). The mean crystallite size of the synthesized nanocomposite was calculated from XRD data using Debye-Scherrer formula equation, equation 12:

$$D = k\lambda / \beta \cos\theta \quad (12)$$

Where D = Crystallite size; k = Scherrer constant (0.94); λ = X-ray wavelength (0.15406nm);

β = Full-width at half maximum of the peak (FWHM); θ = Peak position in XRD graph

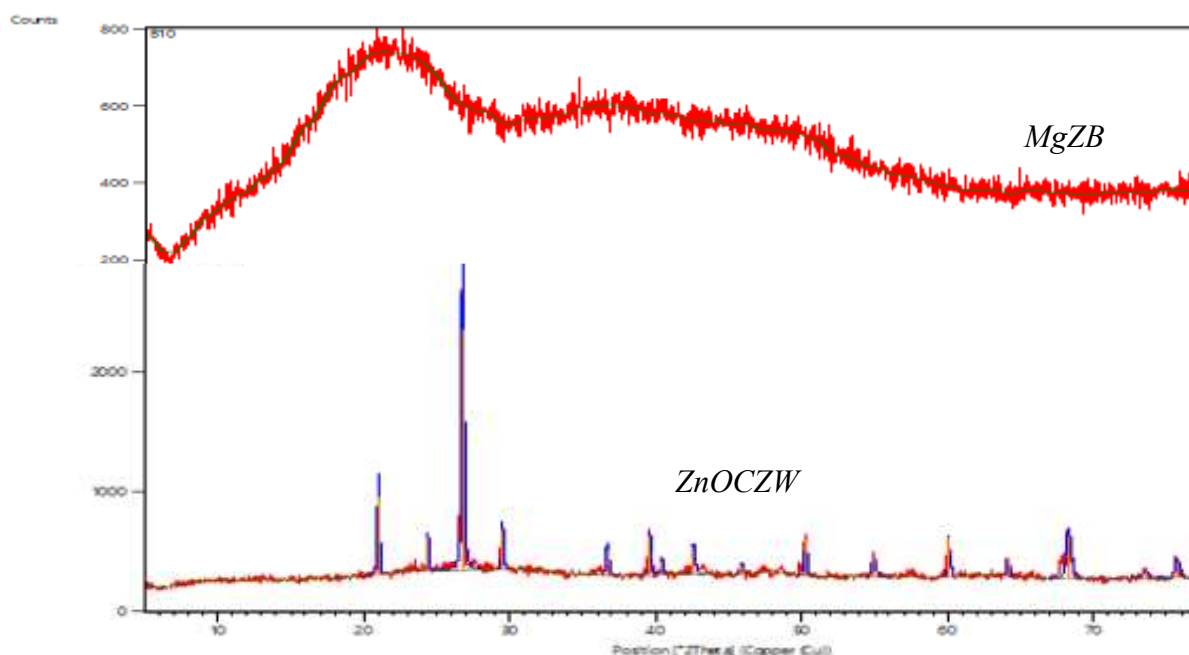


Figure 4: XRD Diffractogram for MgO-ZnO Binary Oxide (MgZBO) nanocomposite and ZnO-Carbonized Zobo (Hibiscus) Waste Nanocomposite (ZnOCZWNC)

The crystallite size (D) calculated from the data obtained from XRD diffractogram using the Debye-Scherrer formula equation was found to be in the range 10.79nm - 111.2nm with an average crystallite size of 40.94 nm for ZnO-carbonized zobo (Hibiscus) waste nanocomposite (ZnOCZWNC) and a range of 25.55nm - 115.73nm with an average crystallite size of 59.42nm was obtained for MgO-ZnO Binary Oxide (MgZBO) nanocomposite.

3.2 Adsorptive Effect of ZnOCZWNC and MgZBO Nanocomposites in Removing Cadmium and Nickel from Contaminated Water

The coefficient of determination (R^2) obtained for adsorption of Ni^{2+} ion and Cd^{2+} ions from contaminated water revealed that there was a goodness of fit of the models applied in interpreting the adsorptive effects of ZnOCZWNC and MgZBO nanocomposites. The R^2 values ranged from 0.66 to 0.96 for Ni^{2+} ions and 0.83 –

0.96 for Cd^{2+} ions (Table 1, Figures 5, 6 and 7). Langmuir adsorption isotherm study of ZnOCZWNC and Mg-Zn Binary oxide for cadmium ion revealed that the adsorbents had the highest sorption capacity of 9.11mg/g and 192.31mg/g respectively, for nickel ions, the maximum sorption capacity were 714.29 mg/g and 416.67 mg/g respectively based on monolayer sorption on a homogeneous surfaces and active sites of the adsorbent with same binding energies. The adsorption intensity (k_L) of ZnOCZWNC and MgZBO nanocomposites for cadmium ions were 0.121 and 0.224 respectively, it corroborated with the maximum sorption capacity of this adsorbents for Cd^{2+} ions. However, the adsorption intensity of ZnOCZWNC and MgZBO nanocomposites for Nickel ions (0.004 and 0.015 respectively) was at variance with the maximum sorption capacity (Table 1). The k_F value of 0.003 and 42.24 for ZnOCZWNC and MgZBO nanocomposites respectively, revealed that MgZBO nanocomposite had a stronger adsorption capacity for cadmium ions, hence confirming its higher maximum adsorption of 192.31mg/g for cadmium ions. Despite the k_F value of ZnOCZWNC and MgZBO nanocomposites for nickel ion were 1.57 and 4.36 for respectively, ZnOCZWNC nanocomposite had a stronger adsorption capacity for nickel ions, hence a higher maximum adsorption of 714.29mg/g for nickel ions. The adsorption intensity (n_F) for cadmium ions on MgZnBO and ZnOCZWNC were 2.66 and 0.20 respectively, indicating that ZnOCZWNC had a higher adsorption intensity, hence a higher maximum adsorption capacity for cadmium ions, likewise, the n_F value for nickel adsorption of 0.79 for Mg-ZnBO and 0.80 for ZnOCZWNC agreed with the fact that ZnOCZWNC had a higher adsorption intensity, hence a higher maximum adsorption capacity for nickel ions. However, only the sorption process of cadmium ions onto MgZnBO was favourable. DRK adsorption isotherm study revealed that the adsorbent - MgZnBO and ZnOCZWNC had the highest sorption capacity of 11.96mg/g as well as 64.24mg/g respectively (Table 1). Likewise, for MgZnBO and ZnOCZWNC the maximum sorption capacity was 795mg/g and 94.72 respectively for cadmium (Table 1). This trend follows the same pattern with that of Langmuir isotherm. DRK adsorption isotherm study revealed that the sorption pattern for cadmium and nickel ions on MgZnBO and ZnOCZWNC was by physical nature or physisorption.

3.3 Langmuir Adsorption Isotherm Study of MgOCZWNC and Mg-Zn Binary oxide for Cadmium and Nickel.

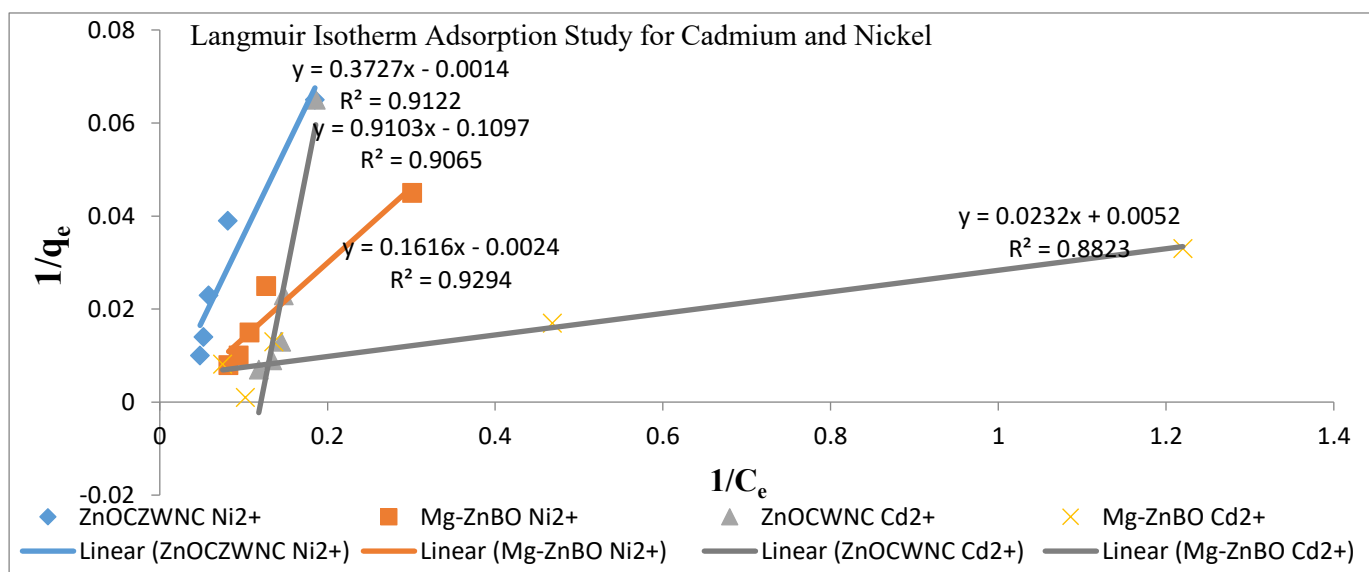


Figure 5: Langmuir Adsorption Isotherm Study of ZnOCZWNC and Mg-Zn Binary oxide for Cadmium and nickel.

3.4 Freundlich Adsorption Isotherm Study of ZnOCZWNC and Mg-Zn Binary oxide for Cadmium and nickel.

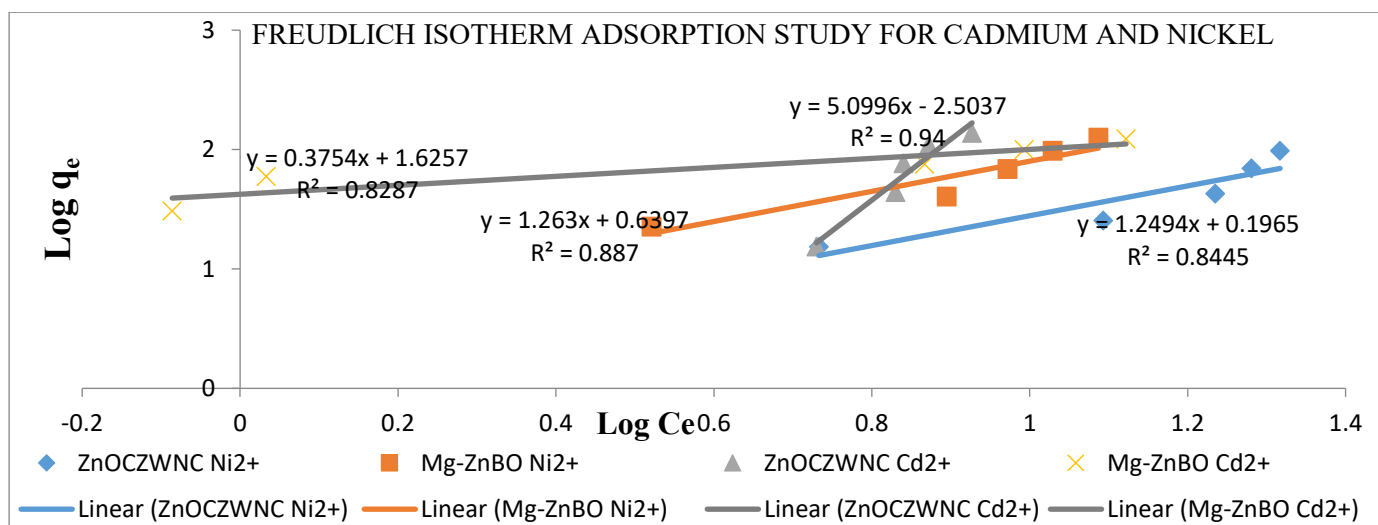


Figure 6: Freundlich Adsorption Isotherm Study of ZnOCZWNC and Mg-Zn Binary oxide for Cadmium and Nickel.

3.5 DRK Adsorption Isotherm Study of ZnOCZWNC and Mg-Zn Binary oxide for Cadmium and Nickel.

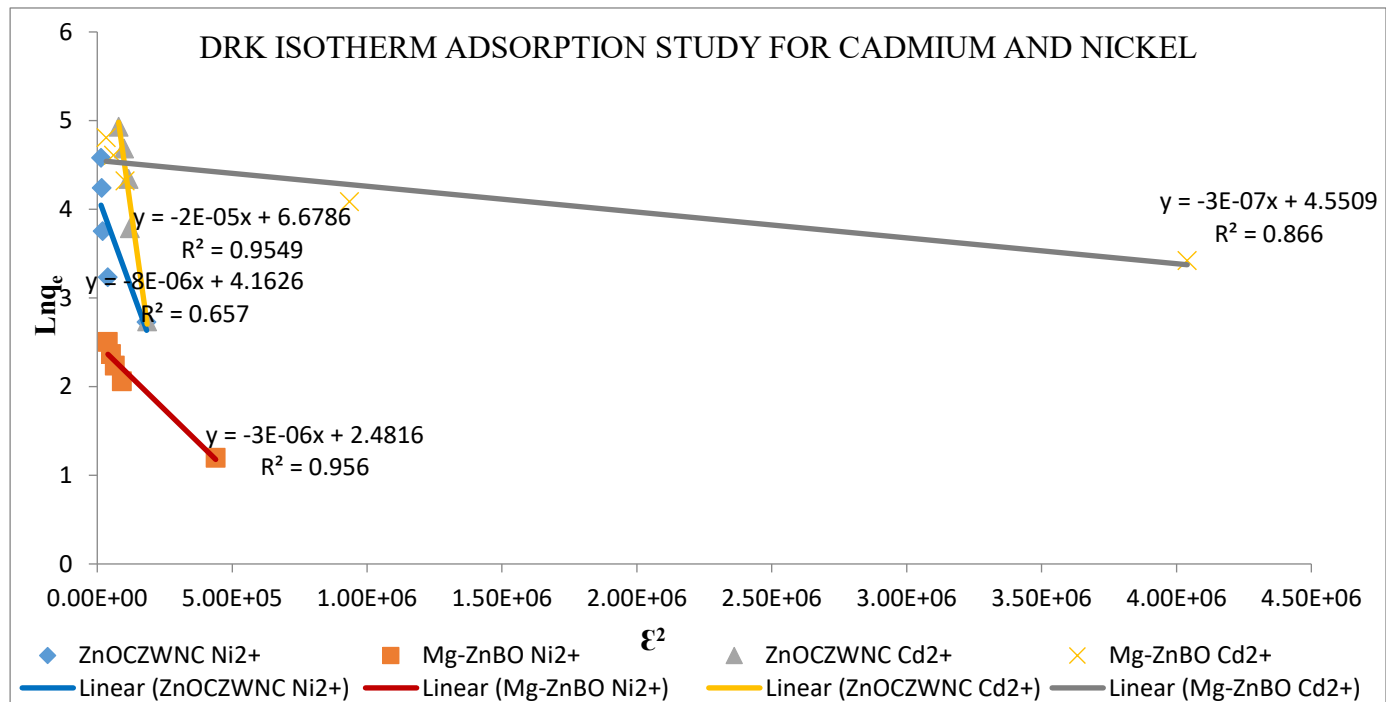


Figure 7: DRK Adsorption Isotherm Study of ZnOCZWNC and Mg-Zn Binary oxide for Cadmium and Nickel.

Table 1: Adsorption Isotherm Model Parameters for Cadmium and Nickel Adsorption

| Adsorption Isotherm Model | Parameters | units | Mg-ZnBO Ni ²⁺ | Mg-ZnBO Cd ²⁺ | ZnOCZWNC Ni ²⁺ | ZnOCZWNC Cd ²⁺ |
|----------------------------|----------------|----------------------------------|--------------------------|--------------------------|---------------------------|---------------------------|
| | | | | | | |
| Langmuir | R ² | - | 0.91 | 0.88 | 0.91 | 0.91 |
| | q _m | mg/g | 416.67 | 192.31 | 714.29 | 9.11 |
| | K _L | L | 0.015 | 0.224 | 0.004 | 0.121 |
| Freundlich | R ² | - | 0.89 | 0.83 | 0.85 | 0.94 |
| | k _F | L/mg | 4.360 | 42.240 | 1.570 | 0.003 |
| | n _F | - | 0.79 | 2.66 | 0.80 | 0.20 |
| Dubinin Radushkevick (DRK) | R ² | - | 0.96 | 0.87 | 0.66 | 0.96 |
| | q _m | mg/g | 11.96 | 795.21 | 64.24 | 94.72 |
| | β | Mol ² /J ² | -3 X 10 ⁻⁶ | -2 X 10 ⁻⁵ | -8 X 10 ⁻⁶ | -3 X 10 ⁻⁷ |
| | E | kJ/mol | 4.083 | 0.100 | 0.250 | 1.034 |

3.6 Aseptic Effect of ZnOCZWNC and MgZBO Nanocomposites on *Staphylococcus aureus* and *Salmonella Typhi* Bacteria Using Turbidimetric Method

The transmitted light from the UV-Vis Spectrophotometer (JENWAY 6320D) revealed there was a sharp rise in the transmitted light for all the nanocomposite within 2hrs, however, the untreated sample displayed a very low light transmittance compared to the samples of staphylococcus and salmonella treated with ZnOCZWNC and MgZBO nanocomposites. This observation indicated there was a steady rise in population of the staphylococcus and salmonella bacteria without any antibacterial interference hence an increase in turbidity whereas the treated samples, experienced a steady decrease in the population of *Staphylococcus* and *Salmonella* after about 2 hrs, due to the aseptic effect of ZnOCZWNC and MgZBO nanocomposites as indicated by a higher light transmittance compared to the untreated (controlled) sample (Figure 8). After about 2 hrs, the samples of staphylococcus and salmonella treated with ZnOCZWNC continued to show a continuous slightly steady rise in transmitted light with time indicating continuity in its aseptic effect at decreasing the population of the bacteria with time. The staphylococcus and salmonella sample treated with MgZnBO experienced a slightly steady decrease in transmitted light after about 2 hrs, indicating a drop in the effectiveness of the nanocomposite after that period. On the over all, the ZnOCZWNC was more efficient in drastically reducing the population of staphylococcus and salmonella in contaminated water (Figure 8).

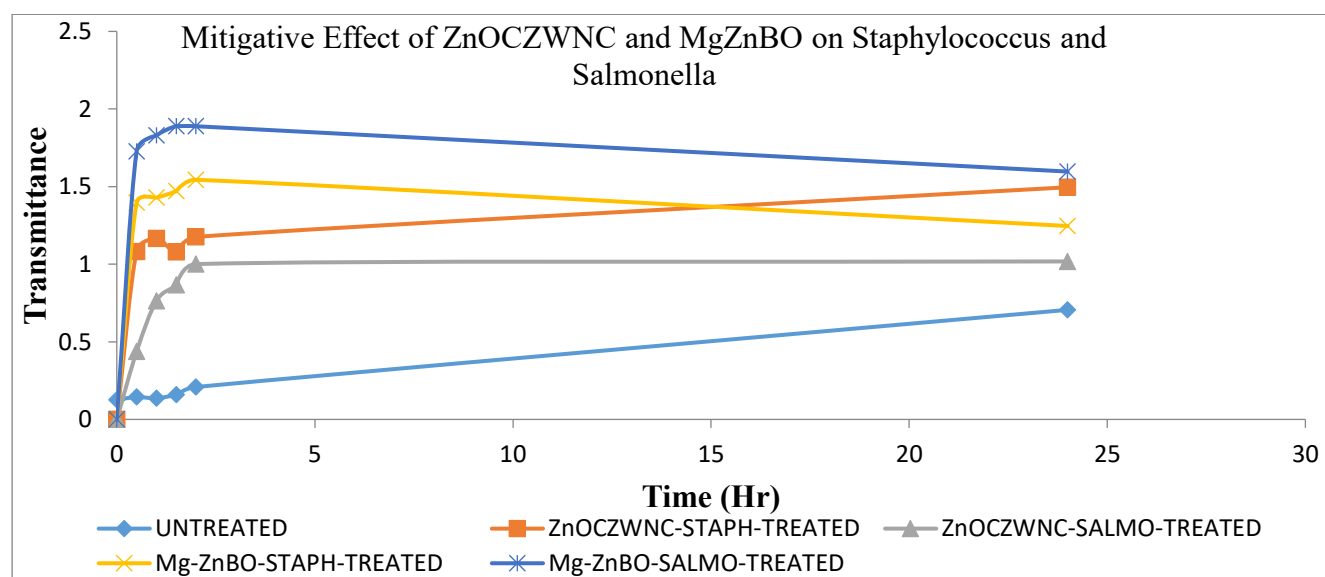


Figure 8: Aseptic Effect of ZnOCZWNC and MgZnBO on *Staphylococcus* and *Salmonella*

4. CONCLUSION

Exploration for a cheaper and better substitute in redeeming our environment of deleterious heavy metals and bacteria is a supreme task that must be achieved. Heavy metals and harmful bacteria has affected the human populace and the economy of our nation, hence the essence of this research work. The average crystallite size of ZnOCZWNC and MgZBO was 40.94 nm and 59.42nm respectively. The ZnOCZWNC adsorbed nickel ions more effectively compared to Mg-ZnBO. Conversely, MgZBO adsorbed cadmium ions more effectively compared to ZnOCZWNC. The adsorption pattern for cadmium and nickel ions onto MgZnBO and MgOCZWNC was by physiosorption. The population of staphylococcus and salmonella in sample treated with ZnOCZWNC and MgZBO nanocomposites experienced a sharp decrease in the first 2 hours compared to the untreated sample. After about 2hrs, the samples of staphylococcus and salmonella treated with ZnOCZWNC show a continuity in its aseptic effect at decreasing the population of the bacteria with time while the staphylococcus and salmonella sample treated with MgZnBO experienced a slight drop in its effectiveness after 2 hours. On the overall, the ZnOCZWNC was more efficient in drastically reducing the population of staphylococcus and salmonella in contaminated water.

CONFLICT OF INTEREST

No conflict of interest was declared by the authors.

REFERENCES

- [1] Ahmed M., Mavukkandy, M. O., Giwa, A., Elektorowicz, M., Katsou, E., Khelifi, O., Naddeo, V. and Hasan, S. W. (2022). Recent developments in hazardous pollutants removal from wastewater and water reuse within a circular economy. *Clean Water*.
- [2] Ambaye, T. G., Vaccari, M., Hullebusch, E. D. V., Amrane, A., and Rtimi, S. (2021). Mechanisms and adsorption capacities of biochar for the removal of organic and inorganic pollutants from industrial wastewater. *International Journal of Environmental Science and Technology*, 18(10), 3273-3294.
- [3] Dewangan, S., Bhatia, A.K., Singh, A.K., and Carabineiro, S.A.C. (2021). Removal of Hydrophobic Contaminants from the Soil by Adsorption onto Carbon Materials and Microbial Degradation. 7, 83.
- [4] Esonu, D. O., Ismail, S., Ajala, A., Yusuf, S. M. and Otolorin, R.G. (2021): Occurrence and Antimicrobial Susceptibility Patterns of Staphylococcus aureus and Salmonella species in Fresh Milk and Milk Products Sold in Zaria and Environs, Kaduna State, Nigeria. *Sahel J. Vet. Sci.*, 18(2), 1-8.

- [5] Faisal, S., Naqvi, S., and Ali, M. (2022) Comparative study of multifunctional properties of synthesised ZnO and MgO NPs for textiles applications. *Pigment & Resin Technology*, 51 (3). pp. 301-308.
- [6] Fwangmun J., Nkemakonam O. C., Adewale O. S., Nabona J., Ntulume I. and Wamyil F. B. (2023). Microbiological quality of water samples obtained from water sources in Ishaka, Uganda. *SAGE Open Medicine*, 11, 1–8.
- [7] Geletu, U. S., Usmael, M. A., and Ibrahim, A. M. (2022). Isolation, Identification, and Susceptibility Profile of *E. coli*, *Salmonella*, and *S. aureus* in Dairy Farm and Their Public Health Implication in Central Ethiopia. *Veterinary Medicine International*, Article ID 1887977, 13 pages. Hindawi.
- [8] Haque, H., Rahman, M., Miah, L., Ahmed, S., Sazib, R. I., Khaton, R., Kabir, A., and Uddin, N. (2021). Exploring Antibiotic Resistance Pattern of *Escherichia coli*, *Salmonella* spp., and *Staphylococcus* spp. Isolated from Eggs in Rajshahi. *European Journal of Agriculture and Food Sciences*, 3(4), July 2021.
- [9] Hassan, H., Iskandar, C. F., Hamzeh, R., Malek, N. J., El Khoury, A., and Abiad, M. G. (2022). Heat resistance of *Staphylococcus aureus*, *Salmonella* sp., and *Escherichia coli* isolated from frequently consumed foods in the Lebanese market. *International Journal of Food Properties*, 25(1), 2435-2444, DOI: 10.1080/10942912.2022.2143521
- [10] Kalarikkandy, A. V., Sree, N., Ravichandran, S., and Dheenadayalan, G. (2022). Copolymer-MnO₂ nanocomposites for the adsorptive removal of organic pollutants from water. *Environmental Science and Pollution Research*
- [11] Kesamsetty, V. R., Singampalli, R., Tadiboyina, A. B., Narasipuram, V. K. P., Venkata, P. K., Manjunatha, H., Ratnakaram, V. N., Sannapaneni, J., Kadiyala, C. B. N. (2022). Role of Carbon Materials in the Removal of Organic Pollutants: An Abridged Review. *Biointerface Research in Applied Chemistry. Platinum Open Access Journal*, 12(2), 1974 – 1997
- [12] Khine, E. E. Koncz-Horvath, D., Kristaly, F., Ferenczi, T., Karacs, G., Baumli, P. and Kaptay, G. (2022). Synthesis and Characterisation of Calcium Oxide Nanoparticles for CO₂ Capture. *J. Nanopart Res*, 24, 139.
- [13] Ku'smierek, K., Kici'nski, W., Norek, M., Pola'nski, M., and Budner, B. (2021). Oxidative and adsorptive removal of chlorophenols over Fe-, N- and S-multi-doped carbon xerogels. *Journal of Environmental Chemical Engineering*, 9 (2021) 105568.
- [14] Moses, O. and Oyibo, O. D. (2022). Effect of Calcium Oxide-Carbonized *Lophira Alata* Sawdust Nanoparticle (COCLASN) in immobilizing

Cadmium and Lead in Contaminated Soil. *Appl. J. Envir. Eng. Sci.*, 8(3), 223-236.

- [15] Naila, K., Faza, L. Z. and Haarstrick, A. (2022). Adsorption of Cd (II) into Activated Charcoal from Matoa Fruit Peel. *Walisongo Journal of Chemistry*, 5(1)
- [16] Rafiq, K., Sani, A. A., Hossain, M. T., Md Hossain, T., Md Hadiuzzaman, Bhuiyan, M. A. S. (2024): Assessment of the presence of multidrug-resistant *Escherichia coli*, *Salmonella* and *Staphylococcus* in chicken meat, eggs and faeces in Mymensingh division of Bangladesh. *Heliyon*, 10 (2024)
- [17] Renu, M. A. and Kailash, S. (2022): Simultaneous removal of heavy metals and dye from wastewater: modeling and experimental study. *Water Science & Technology*
- [18] Subha, V., Divya, K., Gayathri, S., Jagan, M. E., Keerthanaa, N., Vinitha, M., Kirubanandan, S., and Renganathan, S. (2018). Applications of iron oxide nano composite in waste water treatment–dye decolourisation and anti-microbial activity. *MOJ Drug Des Develop Ther*, 2(5), 178–184.
- [19] Ugrina, M., Jurić, A., Nuić, I. and Trgo, M. (2023). Modeling, Simulation, Optimization and Experimental Verification of Mercury Removal onto Natural and Sulfur-Impregnated Zeolite Clinoptilolite—Assessment of Feasibility for Remediation of Mercury-Contaminated Soil. *Processes*, 11, 606.
- [20] Yousefi-Limaee, N., Ghahari, M., Seifpanahi-Shabani, K., Naeimi, A., Ghaedi, S. (2023). Evaluation of Adsorptive Efficiency of Calcium Oxide Nanoparticles for the Elimination of Cationic Dyes: Combustion Synthesis, Adsorption Study and Numerical Modeling Progress in Color Colorants Coating, 16, 1-20.
- [21] Yu, G., Wang X., Liu J., Jiang P., You, S., Ding, N., Guo, Q. and Lin, F. (2021). Applications of Nanomaterials for Heavy Metal Removal from Water and Soil: A Review. *Sustainability*, 13, 7-13.